JOURNAL OF CRITICAL REVIEWS

ISSN- 2394-5125 VOL 07, ISSUE 19, 2020

Broadband communications from ahigh-altitude platform: the European HeliNetprogramme

K Ramakrishna, P Kowmudi, L. Hari Prasad
Assistant Professor[1,2], Associate Professor[3]
Department of ECE,
kramakrishna.ece@anurag.ac.in, pkowmudi.ece@anurag.ac.in, lhariprasad.ece@anurag.ac.in
Anurag Engineering College, Kodada, Telangana

Abstract

In the present climate of growth in bandwidth-hungry telecommunication applications, wireless infrastructure providers are under continuous pressure to exploit the limited radio spectrum as efficiently as possible. In this context, high-altitude platforms (HAPs) are increasingly being cited as having an important role to play in future systems and applications. They have the potential to exploit many of the best aspects of terrestrial and satellite-based systems, while offering advantageous propagation characteristics. Such platforms may be airships or aircraft and for environmental considerations would ideally be solar powered. This paper reviews some of the recent studies under the European HeliNetprogram a consortium-led project to develop a pilotless solar-powered aircraft from which broadband communication services could be supported.

Introduction

Whether treated as a very low satellite or a very tall mast,a vehicle holding a fixed station in the stratosphere may offer an ideal platform from which to support a host of wireless services[1]. The potential spectral efficiency offered in this way is attractive from a number of considerations. For example, cellular architectures may be employed to allow for highly efficient channel reuse schemes, while providing line-of-sight links without the excessive path loss and delay associated with satellite systems. In addition, the many niche applications that have been put forward, such as environmental surveil- lance, traffic monitoring, communications in developing countries and rapid system deployment for disaster relief, to name a few, suggest a tantalising glimpse of the richness of future developments in this field. Apart from these possibilities, the provision of broadband services is expected to be the major economic stimulus to continued platform development. By broadband, we refer here to services akin to LMDS (Local Multipoint Distribution Services), which have been proposed for terrestrial operation in the range 24–29 GHz, or MVDS (Microwave Video Distribution Services), which have been proposed for terrestrial operation typically in the range 40·5–42·5

GHz, in each case delivering multimedia services to the office or home. For HAPs we are considering use of the 47/48 GHz band allocated by the ITU for HAP services, and/or the 28 GHz band. We are also assuming that data rates of at least 2 Mbit/s should be available to the customer. These millimetre-wave bands lead to a require-ment for a line-of-sight link between the customer and the base-station, which for a terrestrial system leads to a large number of base-stations with their associated environ- mental and economic constraints. The HAP broadband network discussed in this paper is a possible solution to these constraints.

High-altitude platforms based on lighter-than-air vehicles[2,3] or conventional aircraft[4] have been proposed and are at various stages of development[5]. The full potential to be offered by unpiloted, solar-powered stratospheric platforms is still a little way off and we review here recent advances in one such research programme while focusing in particular on the platform'sbroadband communications payload.

The European HeliNet project

Pilotless solar-powered aircraft, such as NASA's Centurion programme[6], have been under development

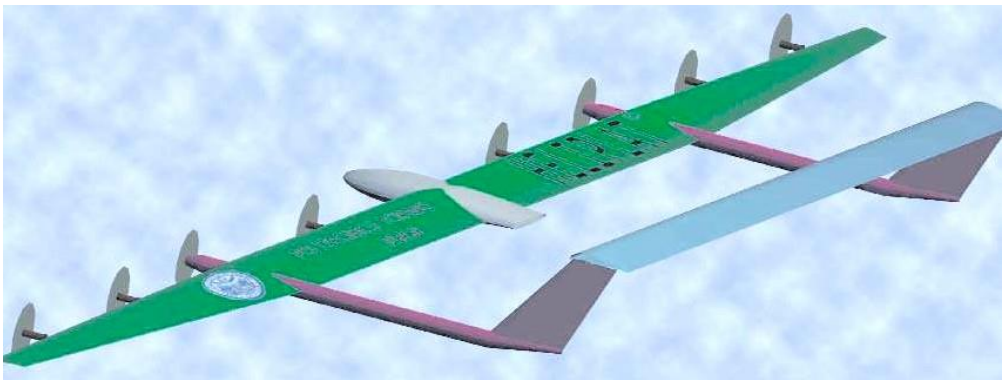

Fig. 1 The HeliPlat high-altitude platform (Design by Giulio Romeo. HeliPlat is a trademark of the Department of Aerospace Engineering, Politecnico di Torino)

for some years. In Europe a similar platform, HeliPlat, is being developed under the HeliNet project[7,8] based on a 70 m wing span aeroplane which would either circle slowly or maintain station at altitudes between 17 and20 km, see Fig. 1. HeliNet is a consortium-led project, funded under an EU 5th Framework Initiative. The project is headed by Politecnico di Torino (Italy), and the University of York (UK) is undertaking the majority of the work on the broadband

ISSN- 2394-5125 VOL 07, ISSUE 19, 2020

telecommunications payload. Recent work on aspects of this payload is presented here.

Spectrum allocations

At present, the spectrum allocated for HAPs worldwide consists of a pair of 300 MHz bands close to 48 GHz, although 28 GHz is also specified in much of Asia. However, a platform at an altitude below 20 km (such as HeliPlat) may be classified as a terrestrial mast and permitted worldwide operation in the latter band; the precise regulatory position is unclear in practice and likely to remain fluid for some time. Bands close to 2 GHz may also be used for UMTS (Universal Mobile Telecommunications System) applications, although this is not considered as part of the present HeliNet 'broadband' payload.

3 Broadband services

To best exploit the spectrum allocated, directive antennas on both the platform and the ground would be utilised to maximise signal-to-noise ratio (SNR) values. Since the dimensions of such antennas may be quite modest (less than 0·5 m aperture diameter), an array of many antennas on the HAP has been proposed to produce a cellular architecture on the ground. As phased-array techniques become less tractable at millimetre wave frequencies,

Table 1: Illustrative downlink data rates at 28 GHz for different types of user. The channel bandwidth is 12·5 MHz and the cell diameter 6 km.

Ground terminal type	Data rate, Mbit/s	Availability, %
Highly portable (100° antenna)	2	99
Fixed (28° antenna)	4	99·9
	12	99
Steered (2° antenna)	10	99·9
	40	99

aperture antennas on the HAP have been proposed as the most efficient means of exploiting bands, particularly at and above 28 GHz. Data rates available to the customer on the ground are strongly dependent on the gain of the ground antenna. Table 1 shows illustrative data rates available for a few scenarios based on link budget calculations; the availabilities dictate the link margin required to overcome rain fade and are based on rain rate statistics.

The platform is expected to maintain station within a position cylinder that is sized depending on the service availability. The target figures for HeliNet are ±4 km laterally and ±1500 m altitude for 99·9% of the time. For the highest data rates, high-gain antennas would be used at the ground terminal, which would need to track the platform's location to minimise pointing losses. The added cost of this mechanism ought not to be too great, since the antennas may be of modest size and weight and a simple tracking algorithm would use as input a control signal from the HAP that included the HAP's displacement. A non-tracking solution would require a wider beam, of which two examples are shown in Table 1: a fully portable antenna and a fixed antenna of 28° beamwidth (this figure is derived from the worst-case angular displacement of the HAP). The data traffic would be backhauled to a number of ground stations using the highest gain antennas practically attainable.

4 Modelling cellular architectures

As part of the study into broadband systems at York, software has been developed to characterise the effect of antenna specifications on the quality of service for various cellular layouts. It is worth drawing attention to some important differences between modelling terrestrial and HAP-based cellular networks. The former are generally interference limited, but the interference levels may be difficult to predict from place to place, being strongly dependent on the effects of terrain and buildings on transhorizon propagation. In contrast, propagation in a HAP-based system is predominantly through free space, with all cells being served from a common point. Although the HAP cellular network will also be inter- ference limited, the interference levels may be predicted (and controlled) with much more confidence due to the favourable propagation conditions. Some results of these prediction techniques will now be pr

ISSN- 2394-5125 VOL 07, ISSUE 19, 2020

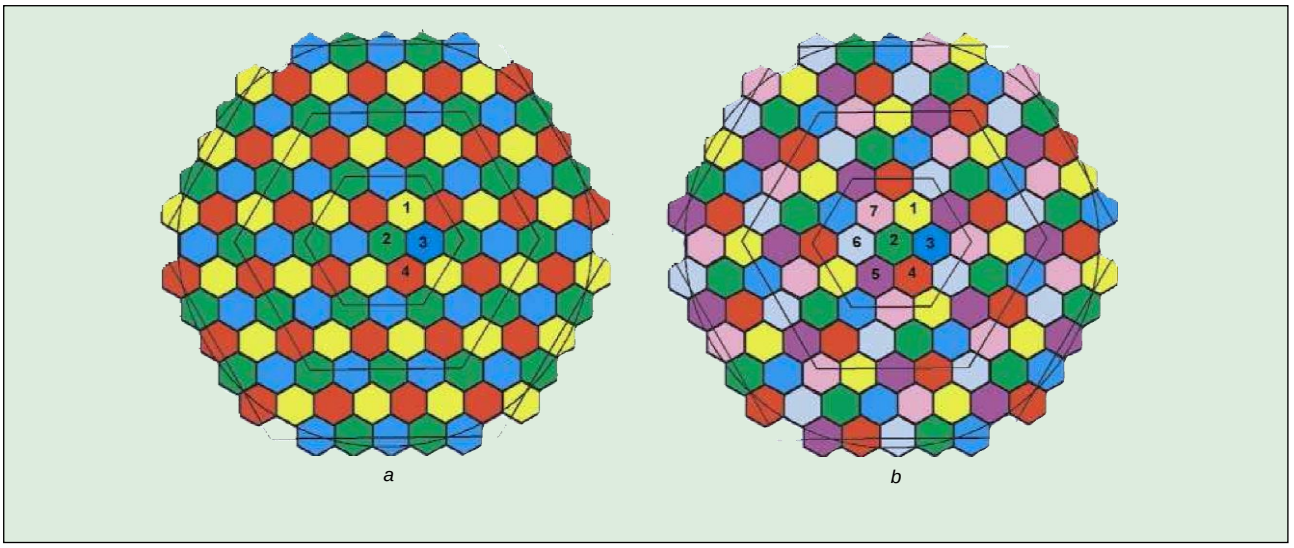

Fig. 2 Channel reuse schemes: (*a*) 4 channels; (*b*) 7 channels

Some selected scenarios have been studied in detail. One of the simplest approaches is to assume circularly symmetric beams and identical antennas illuminating each cell with constant angular separation. In this case, the footprints of the more distant cells become increasingly elliptic and the cells do not tessellate well. Furthermore, the link budget becomes worse with increasing ground distance. In contrast, it has been found that a better approach is to use a conventional, uniform hexagonal cell structure on the ground and select the antenna properties to illuminate the cell in an optimum way. This includes use of an elliptic beam to give a circular footprint on the ground. Also, the directivity is chosen to illuminate the cell edges with maximum power—a similar approach to that taken for satellite antennas where the aperture size may be chosen to maximise the link budget at the edge of the geographical coverage area[9]. In this case, neither the angular spacing of the antennas nor their directivity is constant, and it must be calculated for each cell, but the coverage in terms of carrier-to-interference ratio (CIR) has been found to be better than for constant angular spacing. The CIR is calculated as:

$$CIR = \frac{P_{max}}{\Sigma P_{other}}$$

where P_{max} is the maximum power for the cell of interest and the P_{other} are the interfering powers from the other co-channel antennas. Data arrays of the form $\{x, y, CIR\}$ are generated for each channel, where $\{x, y\}$ are the ground co-ordinates. Depending on the chosen resolution, data array sizes are typically 10 000 elements for each of the co- channel antenna beams. Antenna radiation patterns are modelled using curve fit approximations to minimise processor time. The number of cells may be varied, but the payload limitations of HeliNet have imposed an upper limit in the region of 120.

The software tools developed have provided considerable insight into the interference mechanisms inherent in a HAP-based cellular network. Some examples of recent work are presented below, where a HAP at 17 km height serves a ground area of 60 km diameter so as to limit the elevation angle of the HAP from the ground to around 30°. Fig. 2 shows a layout of 121 hexagonal cells that form concentric 'rings'; the 60 km diameter circle is also shown. Two examples of channel reuse schemes are shown by colour coding.

Although other channel reuse schemes have also been studied, we here concentrate on the 4 and 7 channel cases to illustrate the interference effects in a spot-beam architecture. The CIR patterns

ISSN- 2394-5125 VOL 07, ISSUE 19, 2020

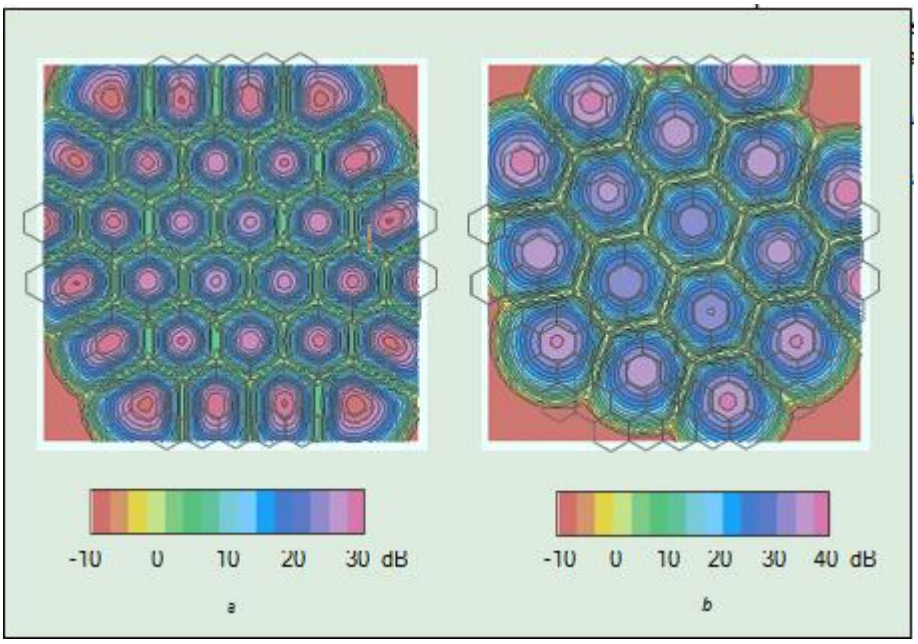

Fig. 3 CIR contours for sidelobes at –50 dB: (*a*) channel 1 of 4; (*b*) channel 1 of 7

for 1 of 4 channels and 1 of 7 channels are shown in Fig. 3. In this case, sidelobes have been modelled as a flat floor whose power level is at 50 dB below the peak antenna directivity. Sidelobes have been identified as being particularly critical to the interference levels, although the angular separation of co-channel cells is of equal importance. Where few channels are reused many times, the cell edges suffer interference from neighbouring main lobes and sidelobe suppression mostly improves CIR values in cell centres only. Where more channels are used and the angular separation between co-channel cells is hence greater, a reduction in sidelobe level reaps gains in CIR over the majority of the coverage area. Such insights are useful in predicting and quantifying the benefits of tighter antenna production specifications.

Returning to Fig. 3, the coverage may also be expressed as a fraction of the co-channel area served at a given CIR threshold value, which is shown in Fig. 4 for the 4 and 7 channel schemes. It can be seen that the CIR begins to roll off at about 20 dB and 30 dB, respectively, for the two reuse schemes. Above these values, geographical cover- age gaps begin to appear in the regions at cell edges, while below these values the cell edges tend to receive multichannel coverage. The steeper roll-off in the 7 channel case is due to the reduced edge-of-cell inter- ference. The tendency for cell edges to be served by more than one channel suggests a useful mechanism for hand- off between channels as the cells move slowly on the ground with any HAP lateral displacement. In a terrestrial cellular system, this level of overlap would require additional base stations, while in the HAP system it is a corollary of the spot-beam architecture.

To further illustrate the distribution of coverage for all cells, Fig. 5 shows plots of power and CIR through the centre of the coverage area. In this case, the sidelobe floor is at –40 dB and the peak CIR values have dropped accordingly. The power profile is applicable to both reuse patterns, since the antenna hardware is the same in each case. The power is scaled as the apparent directivity on the ground, minus the extra free-space loss with respect to the ground point directly beneath the platform.

Fig. 5 again shows the trend apparent in Fig. 3: the centre of the service area tends to exhibit a worse CIR than the outer region. This is due, in part, to the higher absolute sidelobe level of the antennas that serve the outer cells, since they have a higher directivity than those which serve the central region. The free-space loss undergone by the interfering power is also less for the central region than for the outer region, due to the shorter path length. The combined effects of sidelobe power and free-space loss are most detrimental to the central cells.

5 Atmospheric attenuation of millimetre waves

At frequencies below 10 GHz atmospheric losses can largely be ignored, with link budgets being determined essentially by free-space conditions. However, at frequen-cies above 20 GHz absorption and scattering of radiowaves by atmospheric components such as oxygen, watervapour, cloud and rain become increasingly

Rain in particular causes severe attenuation, which may be expressed statistically as in Fig. 6, where the exceedance is the fractional duration for which rain causes a given level of attenuation, and from which link availability is derived. Here, most of the atmospheric attenuation will occur in the first few kilometres above the earth's surface and so standard ITU methods[10] for obtaining satellite–earth atmospheric attenuation statistics may be directly applied to HAPs. (Of course, the use of a HAP offers considerable advantages over a satellite because the free-space path loss and inherent time delay are both much reduced.) Fig. 6 shows the zenith atmospheric attenuation statistics at both 48 GHz and 28 GHz for a platform over Southern Italy. For a link availability of 99·9%, fade margins of 23 dB and 10 dB are required at 48

ISSN- 2394-5125 VOL 07, ISSUE 19, 2020

GHz and 28 GHz, respectively. Hence, for a given fixed power budget, the lower frequency, 28 GHz band offers the greater link availability.

Site diversity

Because the spatial extent of rain cells is limited to a few kilometres, should there be intense rain at a particular site S_1 it is unlikely that for a second site, S_2, a few kilometres away, the rain intensity would be as severe. In this case, it is possible to redirect HAP signals from S_1 to S_2 when heavy rain prevents a direct link being made between the HAP and S_1. The link to S_1 is completed via a terrestrial link between S_2 and S_1. Combining various techniques in the literature[11–13], the predicted improve- ments in fade margin at 48 GHz and 28 GHz at the 99·9% availability level are indicated as a function of site separation in Fig. 7. At a site separation of 20 km, the required fade margins reduce to around 5·5 dB and 2·1 dBat 48 GHz and 28 GHz, respectively.

6 Bistatic scattering from rain

As well as absorbing radiation, rain drops, ice crystals and water droplets in cloud can also degrade link performance by scattering radiation from a volume above its intended destination cell into another cell operating at the same frequency. The geometry of the problem is shown inFig. 8.

The interference power received is calculated by applying the bistatic radar equation to the paths from the transmitter of the unwanted radiation, via each scatterer, to the receiver[14]. Because the phases of the scattered waves reaching the receiver are randomly distributed, the interference power received is effectively the sum of the powers scattered into the receiver from each individual drop or crystal. Thus, for each part of the volume of rain, clouds or snow over the network, the scattering cross- section can be calculated from a knowledge of the scattering cross-sections of the different types of particle and estimations of their number distribution.

In a similar method to that described in Section 4 for calculating co-channel interference for clear air condi- tions, the coverage area is divided into an array of points, or pixels, $\{x, y\}$. At each point of interest $\{x, y\}$, the total interference power due to rain is calculated from the summation of powers scattered away from all the other points $\{i, j\}$ towards the point of interest. The summation includes all co-channel antenna beams with the exception of the beam that illuminates the cell associated with the point of interest and that therefore defines the carrier power.

A map of the CIR can then be drawn up by plotting, at each point, the ratio of power received directly from the carrier, to the total interference power from scattering.

Fig. 9 shows the CIR over the central three concentric rings of the network when a rain event stretches east–west across their centre. The weather front has a nominal 5 km width in which the rain rate is 12 mm/hr, and beyond which the rain intensity falls off exponentially. The channel reuse number is 4 in this case. It can be seen that in general, as in the clear air case shown in Fig. 3, the CIR falls off toward the cell edges, which is expected from the carrier power roll-off due to the illuminating antenna beam. However the CIR peaks do not necessarily coincide with the cell centres because in most cases the rain is not distributed symmetrically around a given cell. In addition, unlike the clear air scenario, the ground-based antenna beam shape now becomes an important factor since scattered power tends to be received through the ground antenna sidelobes. In Fig. 9, a nominal sidelobe level of
–40 dB (below peak) has been used with a 5° beamwidth for the main lobe.

Strategies for ameliorating the detrimental effects of rain scatter are already being suggested. Although any increase in RF transmit power is favourable in overcoming rain attenuation, this does not help reduce interference. Rather, an increase in the channel reuse number will lessen interference by reducing the number of neighbouring co- channel cells affected by the rain event. The adaptation of channel reuse number may be applied dynamically in the region affected by rain alone, while other regions are assigned reuse strategies appropriate for clear air conditions.

Conclusions

The delivery of broadband cellular communication networks from HAPs is continuing to be studied under the European HeliNet programme. The field is still in its infancy and our review has discussed methods of analysis, techniques, and examples of new results rather than attempt a definitive statement of system performance. Although the HeliNet platform will be constrained by limited payload mass and power, the techniques presented here may be readily applied to future HAP communication networks as this exciting technology evolves.

Some of the key issues have been discussed, which particularly include millimetre-wave antennas and propagation, and an estimate of the number of cells that might be supportable by an early platform prototype. The HeliNet consortium has considered the antenna technology best suited to exploit the spectrum, and the dependence of interference, and hence capacity, on the antenna characteristics. An array of
aperture type antennas has been put forward as a means of serving the cells from the platform. For each cell, the antenna directivity may be chosen to illuminate the cell edge with optimum power. Modelling the radiation patterns enables the co-channel interference on theA study of the propagation environment for HAPs, including the effects of rain, is critical to performance evaluation. While the unique properties of a cellular network delivered from a HAP lead to a new set of problems in terms of attenuation and availability, the solutions may also be found within the novelty of the system. These new methods and solutions are made possible by the ability of the system to adapt in real time to changes in both propagation and traffic conditions.

ISSN- 2394-5125 VOL 07, ISSUE 19, 2020

Acknowledgments

This work has been funded under the HeliNet project (IST-1999-11214), part of the EU 5th Framework Initiative.

References

DJUKNIC, G. M., FREIDENFELDS, J., and OKUNEV, Y.: 'Establishing wireless communications services via high- altitude aeronautical platforms: a concept whose time has come?', *IEEE Commun. Mag.*, September 1997, pp.128–135

SkyStation, see http://www.skystation.com

Airship Technologies Group, see http://www.atgplc.com

COLELLA, N. J., MARTIN, J. N., and AKYILDIZ, I. F.: 'The HALO network', *IEEE Commun. Mag.*, June 2000, pp.142–148

TOZER, T. C., and GRACE, D.: 'High altitude platforms for wireless communications', *Electron. Commun. Eng. J.*, June 2001, **13**, (3), pp.127–137

Aerovironment, see http://www.aerovironment.com

ROMEO, G., FRULLA, G,. and FATTORE, L.: 'HELIPLAT: a solar powered HAVE-UAV for telecommunication applica- tions. Design and parametric results. Analysis, manufac- turing and testing of advanced composite structures'. Int. Tech. Conf. on Uninhabited aerial vehicles, UAV 2000, Paris, France, 14th–16th June 2000. See also http:// www.helinet.polito.it

TOZER, T. C., OLMO, G., and GRACE, D.: 'The European HeliNet project'. Airship Convention 2000, Friedrichshafen, July 2000

PRABA, K.: 'Optimal aperture for maximum edge-of- coverage (EOC) directivity', *IEEE Antennas Propag. Mag.*, June 1994, **36**, (3), pp.72–74

ITU-R Recommendation P.618: 'Propagation data and prediction methods required for the design of Earth–space telecommunication systems' (International Telecommunica-tions Union, Geneva, Switzerland, March 2000)

TATTELMAN, P., and SCHARR, K.G.: 'A model for estimating one minute rainfall rates', *J. Clim. Appl. Meteorol.*, 1983, **22**, pp.1575–1580

DRUFACA, G.: 'Radar derived statistics on the structure of precipitation patterns', *J. Appl. Meteorol.*, 1977, **16**, Pt. 10, pp.1029–1035

KONEFAL, T., WATSON, P. A., SHUKLA, A. K., and AKRAM,
A.: 'Prediction of monthly and annual availabilities on 10–50 GHz satellite–Earth and aircraft-to-aircraft links', *IEE Proc., Microw. Antennas Propag.*, April 2000, **147**, (2), pp.122–127

SPILLARD, C., THORNTON, J., GRACE, D., and TOZER, T.: 'Calculation of interference levels due to rain scatter on high-altitude platform links'. ICAP 2001, 11th Int. Conf on Antennas and Propagation, Manchester, UK, 17th–20th April 2001, IEE Conf. Publ. No. 480, **2**, pp.632–636

.